P8.1

Hurricane and Tropical Cyclone Tornado Environments from RUC Proximity Soundings

Jonathan M. Davies*
Private Meteorologist, Wichita, Kansas

1. Introduction

Studies such as those by McCaul (1991, 1996) have examined thermodynamic and kinematic characteristics of landfalling hurricane and tropical cyclone environments associated with shallow supercells and tornadoes using observed and simulated soundings. With high resolution model soundings available to forecasters in recent years as estimates of near-storm environment, a study based on operational model-derived profiles and their characteristics associated with tropical cyclone tornado settings has been absent, but would seem desirable.

Over 100 analysis profiles from the Rapid Update Cycle (RUC) associated with tropical cyclone events during 2001-2006 were archived. These profiles were used to see if there are some detectable differences in characteristics between nontornadic and tornadic tropical cyclone environments when examining accepted supercell tornado forecast parameters via model-derived soundings. Informal results will be shown and discussed, followed by some brief case studies applying these results.

2. Database and methodology

A database of over 1500 RUC analysis profiles associated with severe weather events during 2001-2006 was expanded from Davies (2004 and 2006), and included 109 profiles associated with tropical cyclones. These 109 profiles were linked to 21 landfalling hurricanes and tropical cyclones along the Gulf and Atlantic coasts of the United States. All profiles were located within 100 km and 60-90 min prior to tornado-warned storms from radar, or storms yielding reported tornadoes, and were located to the east or southeast of the associated storms to approximate the inflow air mass. The profiles were also updated in the lowest levels using observed surface data, as in Davies (2004). Tornado reports were verified from the publication *Storm Data* and, in a few recent cases, the Storm Prediction Center (SPC) storm report log.

Corresponding author address:
Jonathan M. Davies
3206 N. Westwind Bay e-mail: jdavies1@cox.net
Wichita, KS 67205 http://members.cox.net/jdavies1

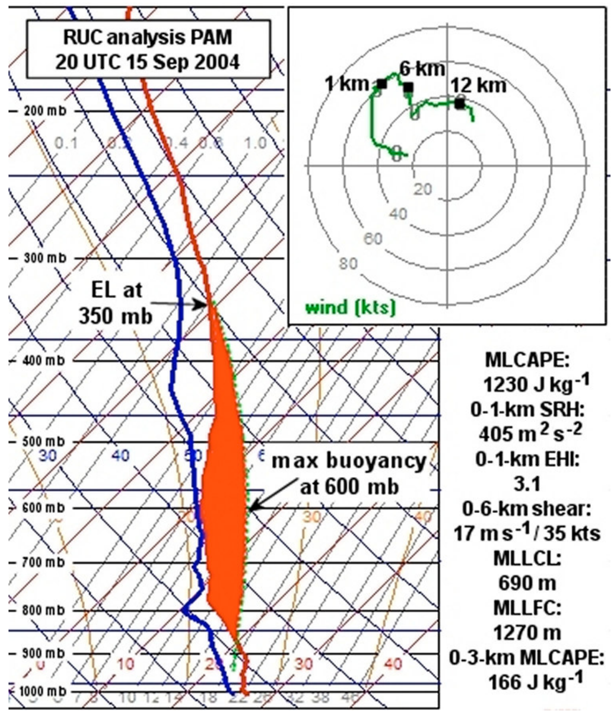

Fig. 1. *SkewT-logp diagram and hodograph of RUC analysis sounding for Panama City (Tyndall A.F.B.), Florida at 2000 UTC 15 Sep 2004 in the right front quadrant of Hurricane Ivan. Red line is temperature, blue line is dewpoint, and red shading is lowest 100-mb mixed-layer CAPE. Significant features are labeled.*

Most of the 109 profiles were in the right front quadrant of tropical cyclones, with 68 associated with tornadic storms, and 41 associated with nontornadic tornado-warned storms. All but one of the tornadic storms was in the right front quadrant.

McCaul (1991) found some characteristics of soundings associated with supercell storms in tropical cyclones (e.g., relatively shallow buoyancy and very strong low-level shear as in Fig. 1) to be notably different from supercell profiles in the Great Plains. However, his study also showed that important supercell tornado parameters such as shear and helicity were maximized in the right front quadrant of tropical cyclones where most tornadoes occur. For this study, parameters known to be important from empirical studies about general supercell tornado environments

Table 1. Selected median parameter values for RUC database supercell cases associated with hurricanes and tropical cyclones

RUC tropical cyclone supercell cases	MLCAPE J kg^{-1}	0-1-km SRH m^2 s^{-2}	0-1-km EHI	0-6-km shear m s^{-1}	MLLCL m	MLLFC m	0-3-km MLCAPE J kg^{-1}
Lowest 100-mb mean parcel:							
F2-F4 sig tor (23 cases)	996	293	1.6	20	754	1131	121
F0-F1 wk tor (45 cases)	732	206	0.8	18	722	1043	100
nontornadic (41 cases)	557	186	0.6	15	819	1455	62
Lowest 50-mb mean parcel:							
F2-F4 sig tor (23 cases)	1232	293	2.1	20	536	963	145
F0-F1 wk tor (45 cases)	917	206	1.2	18	480	825	141
nontornadic (41 cases)	718	186	0.7	15	611	1203	82

(e.g., Davies and Johns 1993; Rasmussen and Blanchard 1998; Rasmussen 2003; Thompson et al. 2003; Davies 2004, Craven and Brooks 2004) were computed for the RUC tropical cyclone profiles. Tornadic tropical cyclone events were compared with nontornadic events to find parameters that appeared to discriminate between groupings. All thermodynamic parameters were computed using mixed-layer (ML) lifted parcels from the lowest 100 mb or lowest 50 mb, incorporating the virtual temperature correction (Doswell and Rasmussen 1994).

3. Results

Table 1 shows median values of several parameters commonly used in supercell tornado forecasting, computed for the tropical cyclone RUC profiles using lowest 100-mb mixed-layer lifted parcels. These are grouped by nontornadic, weak tornadic (F0-F1 intensity), and significant tornadic (F2+ intensity). Significant differences in total convective available potential energy (CAPE), low-level storm-relative helicity (SRH), and deep layer shear are seen in the first half of Table 1. Comparing just the significant tornadic with nontornadic cases, median total CAPE was more than 70% larger, median 0-1-km SRH was more than 50% larger, and median 0-6-km shear was a third larger for profiles associated with significant tornadoes in tropical cyclones.

Combinations of CAPE and SRH via the energy-helicity index (EHI, e.g., Davies 1993; Rasmussen 2003) were also greater for significant tornadoes in the first part of Table 1. The median 0-1-km EHI for F2+ intensity tornadoes was fully 170% larger than that for the nontornadic cases. Figure 2 shows the distribution of 0-1-km EHI between nontornadic and significant tornadic tropical cyclone cases (weak tornadoes were omitted to emphasize differences), confirming that larger CAPE-SRH combinations in tropical cyclones tend to be associated with stronger tornadoes.

Low-level thermodynamic parameters, such as lifting condensation level (LCL), level of free convection (LFC), and CAPE below 3 km (0-3-km CAPE), are also shown in Table 1. With LCL and LFC heights generally quite low and 0-3-km CAPE sizable for all groupings, these parameters reflect the very moist and humid low-level conditions present in tropical cyclones.

Because near-saturated conditions are typical of tropical cyclones, it is worth considering parameters

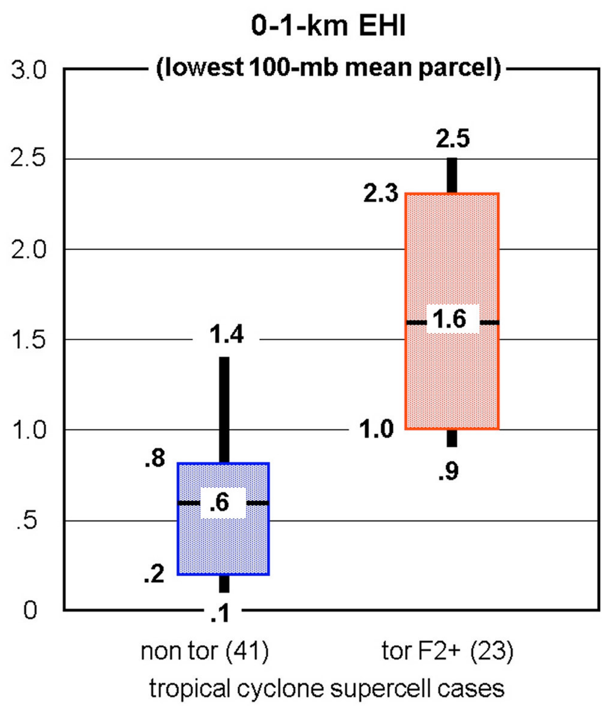

Fig. 2. *Box and whisker diagram showing distribution of 0-1-km EHI for tropical cyclone supercells in RUC database that were nontornadic (41 cases) and significant tornadic (23 cases). Boxes are 25th to 75th percentiles, and whiskers extend to 10th and 90th percentiles. Horizontal bars show median values.*

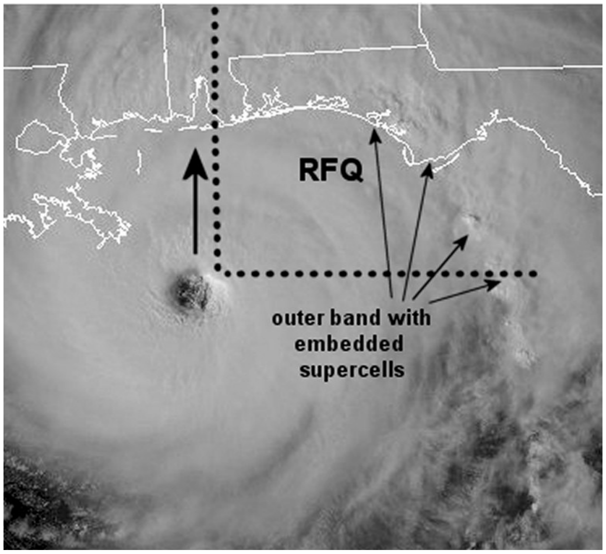

Fig. 3. *Visible satellite image of Hurricane Ivan at 2045 UTC 15 Sep 2004. Relevant features are indicated. Heavy arrow is direction of movement. "RFQ" is right front quadrant, between dotted lines.*

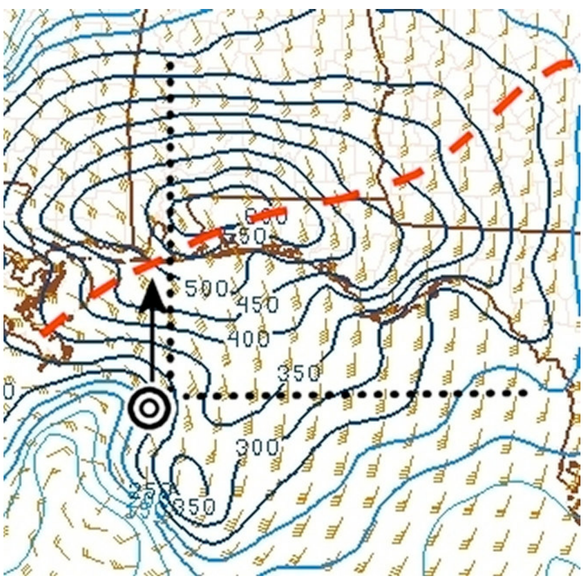

Fig. 4. *SPC mesoanalysis of 0-1-km SRH (m^2 s^{-2}) at 2000 UTC 15 Sep 2004, other features as in Fig. 3. Hurricane eye is double circle. Dashed red line is important thermal boundary.*

computed using lifted parcels from a shallower mixed-layer. Moist tropical cyclone conditions suggest that lowest 100-mb mean lifted parcels (commonly used) may average too deep a mixed layer to properly reflect relevant CAPE values when very large low-level humidity is present. The second half of Table 1 shows median thermodynamic parameter values using mean lifted parcels from the lowest 50 mb. For significant tornadoes, total CAPE increased noticeably (median value > 1000 J kg^{-1}) as did 0-1-km EHI (median value

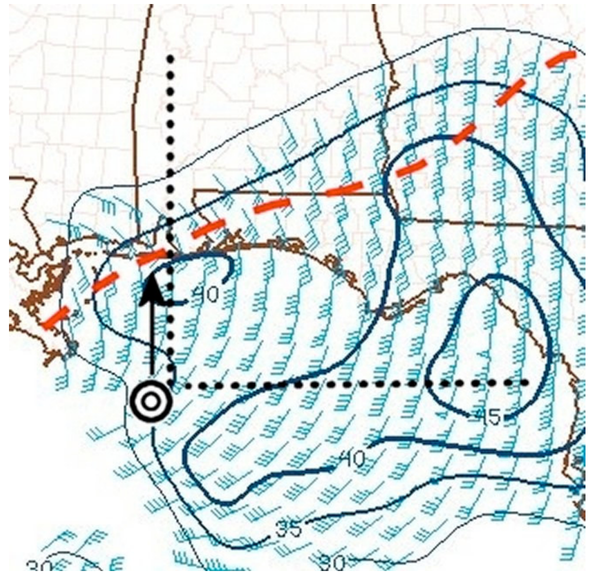

Fig. 5. *As in Fig. 4, except 0-6-km shear (kts).*

> 2.0). With the near saturated conditions in tropical cyclones, it is possible that the second half of Table 1 may be more representative of true parameter values and environment characteristics.

The next section will look at some brief case studies, applying the results in this section to tornadic and nontornadic landfalling tropical systems using parameter fields from the SPC mesoanalysis (Bothwell et al. 2002), which uses mixed-layer lifted parcels from the lowest 100 mb.

4. Case Studies

a. Hurricane Ivan – 15 September 2004

Hurricane Ivan produced more than 20 tornadoes in the Florida panhandle and southwest Georgia on the afternoon and evening of 15 September 2004 before and during landfall. Six deaths, 16 injuries, and more than $13 million in damage resulted from these tornadoes.

Figure 3 is a satellite image of Ivan at mid afternoon on the 15th, with important features indicated. Figs. 4 and 5 show SPC mesoanalysis fields of 0-1-km SRH and 0-6-km shear, respectively. From these analyses, a large area of strong low-level SRH (> 400 m^2 s^{-2}) and deep layer shear (> 20 m s^{-1} or 40 kts) was present in the right front quadrant of Ivan. Onshore surface flow also contributed to mixed-layer CAPE that was sizable over much of the Florida panhandle (1000-1800 J kg^{-1}, not shown). This resulted in large CAPE-SRH combinations (0-1-km EHI > 4.0, Fig. 6) that extended well in advance of Ivan, deep into the right front quadrant, suggesting potential for low-level mesocyclones and possible tornadoes.

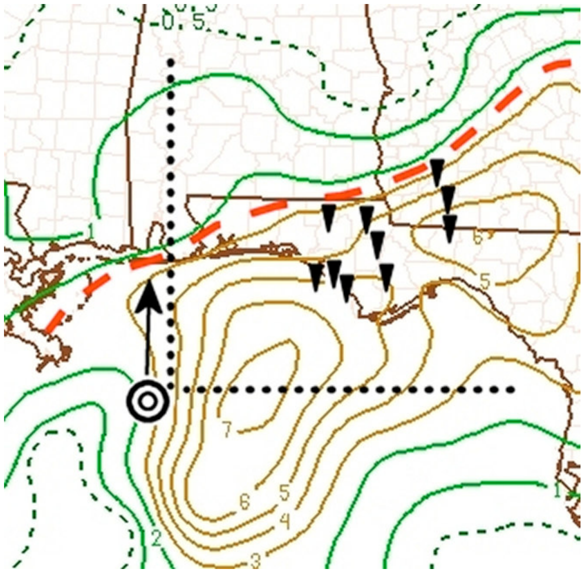

Fig. 6. *As in Fig. 4, except 0-1-km EHI. Solid inverted triangles are locations of F1-F2 tornadoes (6 deaths) during afternoon and evening of 15 Sep 2004.*

In Figs. 4 through 6, a thermal boundary (dashed red line) is shown over Georgia and the Alabama-Florida border. This boundary had moved onshore in advance of Ivan, ushering in a broad tropical air mass across the Florida panhandle. With the juxtaposition of significant CAPE, large low-level SRH, and deep layer shear within Ivan's right front quadrant as it moved inland, conditions were very favorable for tornadoes based on the RUC profile results from the prior section (also see Fig. 1 earlier). Tornadoes in the Panama City area after 2000 UTC killed 2 people, and later tornadoes further inland resulted in additional deaths. Over the following 2 days, the inland remains of northeastward-moving Ivan retained strong shear and CAPE characteristics (not shown) that were well-depicted on SPC mesoanalysis graphics. The result was many additional tornadoes from Georgia to Virginia.

b. Hurricane Dennis – 10 July 2005

Although smaller, Hurricane Dennis on 10 July 2005 had some similarities to Ivan in that it was a category 4 hurricane shortly before landfall and came onshore in the same area from the same general direction. However, in contrast to Ivan, Dennis was not a prolific tornado producer.

Figure 7 is a composite radar image of Dennis shortly after landfall on 10 July 2005, with relevant features indicated. In contrast to Ivan, tropical air was *lagging behind* the right front quadrant (note the boundary position in Fig. 8, dashed), and was having difficulty replacing the cooler air mass over Georgia and Alabama. The 0-1-km SRH and 0-6-km shear

Fig. 7. *Composite radar reflectivity image of Hurricane Dennis at 1950 UTC 10 July 2005. Relevant features are indicated, with heavy arrow, dotted lines, and "RFQ" similar to Fig. 3.*

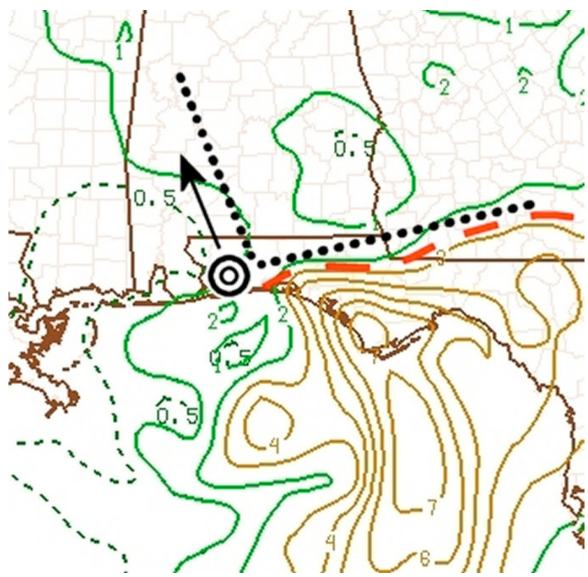

Fig. 8. *As in Fig. 6, except at 1900 UTC 10 July 2005. Dashed red line is important thermal boundary trailing the right front quadrant of Hurricane Dennis.*

fields (not shown) were very similar to Ivan in pattern and magnitude over the right front side of Dennis, with SRH > 400 m^{-2} s^{-2} and deep shear > 20 m s^{-1} (40 kts). However, unlike Ivan, these characteristics were juxtaposed over a cooler air mass with much less CAPE (not shown, 250-500 J kg^{-1}). Figure 8 (0-1-km EHI) shows that combinations of CAPE and SRH were sizable in Dennis' *right rear* quadrant, but not in the important right front quadrant where both SRH and deep layer shear were maximized. This unfavorable

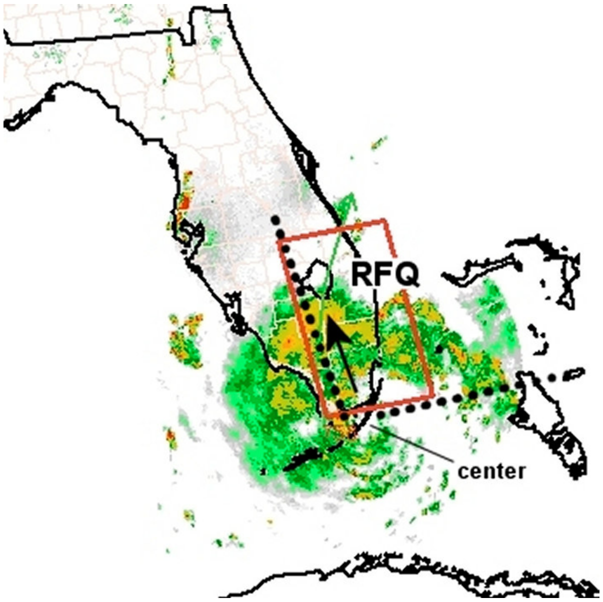

Fig. 9. *Composite radar reflectivity image of tropical storm Ernesto at 0118 UTC 30 Aug 2006. Relevant features are indicated, similar to Fig. 3 and Fig. 7. Red box is tornado watch.*

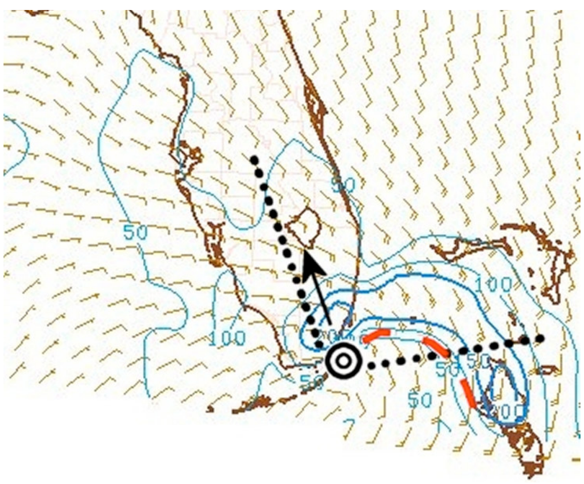

Fig. 10. *SPC mesoanalysis of 0-1-km SRH (m^2 s^{-2}) at 0100 UTC 30 Aug 2006. Additional features are similar to Fig. 4, including thermal boundary.*

arrangement of environment characteristics relative to Dennis' right front quadrant was probably a major reason only 1 or 2 tornadoes occurred (F0 intensity, not shown) in the far eastern Florida panhandle.

c. Tropical storm Ernesto – 29 August 2006

After a brief period as a hurricane, Ernesto crossed Cuba and made landfall in southeast Florida as a tropical storm on the evening of 29 August 2006. A tornado watch (Fig. 9) was in effect over Ernesto's right front quadrant, but no tornadoes were reported,

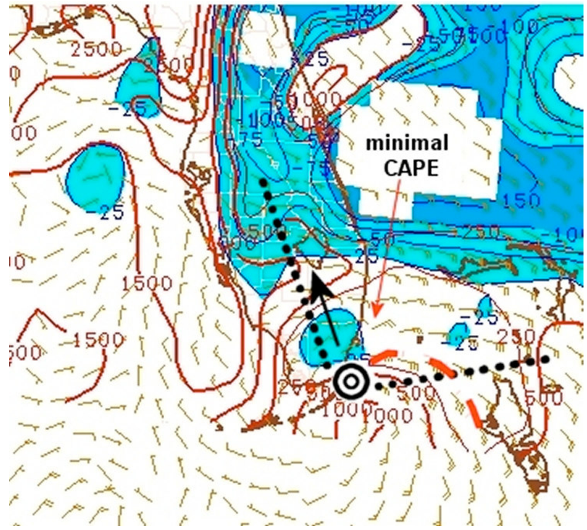

Fig. 11. *As in Fig. 10, except mixed-layer CAPE (red contours, J kg^{-1}) and CIN (blue shading > 25 J kg^{-1}). Wind barbs are surface winds.*

although *Storm Data* was yet to be finalized at the time of this paper.

Figure 9 shows a composite radar reflectivity image of Ernesto at landfall shortly after 0100 UTC on 30 August 2006, with relevant features indicated. Although 0-1-km SRH (> 200 m^{-2} s^{-2}, Fig. 10) was maximized over Ernesto's right front quadrant ahead of a weak wind shift and thermal boundary, mixed-layer CAPE was weak (< 250 J kg^{-1}, Fig. 11) in the same location. As a result, CAPE-SRH combinations (0-1-km EHI < 0.5, Fig. 12) were poor over south Florida, with larger values (> 1.0) remaining offshore. Also important, 0-6-km shear (Fig. 13) was weak, with values less than 15 m s^{-1} (30 kts) over Ernesto's right front quadrant. This lack of deep layer shear, and the poor arrangement of other environment characteristics in this case were probably a significant contributor to the absence of tornadoes during the Florida landfall of Ernesto.

Two evenings later, Ernesto made a second landfall in North Carolina after moving back out over the Atlantic Ocean. By this time, SRH and deep layer shear characteristics (not shown) had improved in combination with adequate CAPE over Ernesto's right front quadrant. These factors may have helped in the generation of a few tornadoes along the North Carolina coast on 31 August 2006.

5. Summary

Tornadoes are almost always a possibility with landfalling tropical cyclones, particularly in the right front quadrant (e.g., Pearson and Sadowski 1965). In this study, 17 of 21 such systems produced at least 1

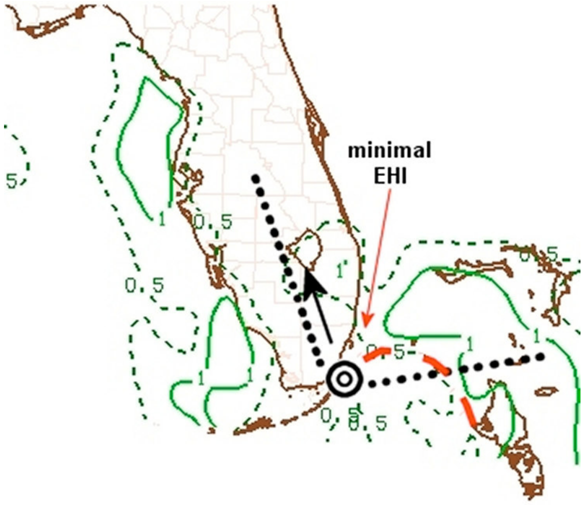

***Fig. 12.** As in Fig. 10, except 0-1-km EHI.*

***Fig. 13.** As in Fig. 10, except 0-6-km shear (kts).*

tornado. The results from the RUC soundings in this study show that, although tropical cyclone environments are notably different from other supercell tornado environments (McCaul 1991), accepted supercell forecasting parameters from model-derived soundings are often useful in helping to determine hurricane and tropical cyclone systems more likely to produce tornadoes.

In particular, the juxtaposition of increased values of 0-1-km SRH, 0-6-km shear, and CAPE-SRH composites such as the 0-1-km EHI *in the right front quadrant* of tropical cyclones can highlight tropical systems that will be more prolific tornado producers. As shown in the case studies from section 4, the use of these parameters in combination with careful analysis of air masses and boundaries (e.g., Edwards and Pietrycha 2006, this volume) within the right front quadrant can be helpful operationally for locating areas of increased tornado potential. Parameters such as LCL height, LFC, and 0-3-km CAPE are probably less useful as distinguishing factors because the large humidity in tropical cyclones usually results in low-level thermodynamic characteristics that are fairly uniform from case to case, unlike non-tropical supercell settings.

Future research might focus on choice of lifted parcel when computing thermodynamic parameters in humid and near-saturated environments, such as those associated with hurricanes and tropical cyclones. The second half of Table 1 from section 3 suggests that shallower mixed-layer depths (such as the lowest 50 mb, instead of the lowest 100 mb) could be more appropriate for computing relevant CAPE and related parameters in such settings. This is somewhat similar to findings by Guyer and Davies (2006, this volume) who found near-surface lifted parcels more relevant for computing CAPE close to cold core 500-mb lows. Given the very moist low-level conditions that limit low-level mixing and dilution of buoyancy in tropical cyclones, this issue probably warrants further investigation.

Key references (other references available on request)

Bothwell, P. D., J. A. Hart, and R. L. Thompson, 2002: An integrated three-dimensional objective analysis scheme in use at the Storm Prediction Center. Preprints, *21st Conf. on Severe Local Storms*, San Antonio, TX, Amer. Meteor. Soc., J117-J120.

Davies, J. M., 1993: Hourly helicity, instability, and EHI in forecasting supercell tornadoes. Preprints, *17th Conf. on Severe Local Storms*, St. Louis, MO, Amer. Meteor. Soc., 107-111.

-------., 2004: Estimations of CIN and LFC associated with tornadic and nontornadic supercells. *Wea. Forecasting*, **19**, 714-726.

-------, 2006: Tornadoes in environments with small helicity and/or high LCL heights. *Wea. Forecasting*, **20**, 579-594.

Edwards, R., and A. E. Pietrycha, 2006: Archetypes for surface baroclinic boundaries influencing tropical cyclone tornado occurrence. Preprints, *23rd Conf. on Severe Local Storms*, St. Louis, MO, Amer. Meteor. Soc., this CD-ROM.

Guyer, J. L., and J. M. Davies, 2006: Environment characteristics associated with tornado events near closed cold core 500-mb lows. Preprints, *23rd Conf. on Severe Local Storms*, St. Louis, MO, Amer. Meteor. Soc., this CD-ROM.

McCaul, E. W., 1991: Buoyancy and shear characteristics of hurricane-tornado environments. Mon. Wea. Rev, **119**, 1954–1978.

-------, E.W., Jr. and M. L. Weisman. 1996: Simulations of shallow supercell storms in landfalling hurricane environments. *Mon. Wea. Rev*., **124**, 408–429.

Pearson, A. D. and A. F. Sadowski, 1965: Hurricane-induced tornadoes and their distribution. *Mon. Wea. Rev.*, **93**, 461-464.

Rasmussen, E. N., 2003: Refined supercell and tornado forecast parameters. *Wea. Forecasting*, **18**, 530-535.

Thompson, R. L., R. Edwards, J. A. Hart, K. L. Elmore, and P. Markowski, 2003: Close proximity soundings within supercell environments obtained from the Rapid Update Cycle. *Wea. Forecasting*, **18**, 1243-1261.